VIBRATIONS OF SOIL AND FOUNDATION DUE TO RAILWAY, BLAST AND IMPACT LOADING

L. Auersch

BAM Federal Institute
of Materials Research
and Testing,
Unter den Eichen 87,
12200 Berlin,
Germany.
lutz.auersch-saworski@bam.de

The vibrations of soil and foundations are demonstrated for different types of loading. Train-induced ground vibrations are studied in a measurement campaign where a test train has run with regularly varied speeds. The measured train-induced soil vibration at 2 to 100 m distance from the track is compared with the wave propagation due to hammer excitation and with the theoretical wave field. The strong influence of the soil and the train speed on the amplitudes and frequencies of the vibration has been analysed for passages of the locomotive and the carriages. - The generation of ground vibration by strong explosions has been studied on a large testing area with sandy soil. The propagating waves were measured in a regular grid of measuring points in 10 to 1000 m. Therefore, the dominance of certain waves at certain distances and the changes of compressional waves and Rayleigh waves could clearly be observed. The results are compared with impulse hammer measurements in the range of 5 to 50 m. - A drop test facility has been built on the testing area of the Federal Institute of Materials Research and Testing (BAM). Heavy masses (containers) of up to 200 t can be dropped from 10 m height on a big reinforced concrete foundation. The foundation was instrumented by accelerometers, strain gauges and pressure cells to give information about the loading condition and by geophones to measure the vibration of the surrounding soil and building. Both excitation processes, the release of the mass and the impact, produce high vibration amplitudes. On a smaller drop foundation, the influence of the drop height and the target stiffness has been studied more systematically.

Keywords: Ground vibration; train passage; explosion; mass drop; amplitude-distance law, filter effect of the soil; train speed; blasting charge; drop height; target stiffness

1 Introduction

Heavy machines, traffic or other industrial activities yield dynamic loads which excite the foundation, waves through the soil and nearby buildings. These dynamic loads can cause annoyance and damage. In the basic book of Barkan [1] and later in [2], many industrial examples and the design of foundations, namely for impact loads have been given. Vibro-acoustic problems of machines and pipelines are presented for example in [3 - 5]. This contribution focuses on extreme excitations of ground and building vibrations. The phenomena of different ground vibrations have been analysed by many measurements. Basically, the time histories of the particle velocities have been analysed. The maxima as a function of the distance from the source yield amplitude-distance laws [6, 7]. The travel time from sensor to

sensor results in the wave velocity. The spectra or frequency-dependent transfer functions are used to characterize the soil structure at the measuring site [8 - 10]. Finally, the measured amplitudes are related to the excitation parameters, the blasting charge, the drop height, or the train speed. If the train speed reaches the wave velocity of the soil, very high amplitudes are predicted in theory [11, 12], but this is rarely found in reality. Usually, the railway excitation is rather low compared to the blast and impact loading. The influence of the heavy locomotive compared to the light-weight carriages will be shown. Experimental campaigns are important to understand the train-track-soil interaction [13 – 20].

The material is presented as follows. The contribution starts with railway vibration, followed by blast vibration. Finally, mass drops are analysed systematically in small scale tests and a heavy mass drop is studied in detailed measurements.

2 Ground vibration due to railway traffic

Vibration due to railway traffic is a research field of BAM since 40 years. As an example, results of a very complex measuring campaign [14] are shown where vehicle, track and soil vibrations have been measured simultaneously at a surface, bridge and tunnel line (fig. 1). The characteristics of the vibrations at different measuring points are demonstrated in figure 2. At the rail (or sleeper, fig. 2a), the passage of every axle can be observed clearly. At 2 m distance from the track (fig. 2b), the axle impulses can still be traced back, but they are completely lost at 10 m distance at the latest (fig. 2c). A stationary vibration of many frequencies can be found there as in most measuring points of the mid field. The far field (r = 100 m, fig.2d) is still stationary, but only with a narrow frequency band (around 12 Hz for this specific site).

The site specific effects are analysed by the transfer functions of the soil which is calculated by wave number integrals [9, 10] and measured by hammer impacts (fig. 3). The soil of this site has a certain cut-on frequency at about 10 Hz due to a stiff sub-soil in 10 m depth and a certain high cut-off frequency due to the material damping which is found to be more pronounced in the measurements (fig. 3a).

The measurements of train passages with different speeds have been analysed by one-third octave band spectra. Figure 4a-e shows the ground vibration during the passage of the locomotive. The spectra of the soil vibration for different train speeds show typical frequency ranges of railway excitation. Clear peaks can be found at 32, 40 and 50 Hz for 60, 80 and 100 km/h which are due to the sleeper distance excitation [15]. At the near-field point, the low-frequency spectrum is due to the passage of the static axle loads. There is another important frequency range at 12 – 16 Hz which is dominant at the far-field. The whole ground vibrations are rather constantly concentrated between 10 and 60 Hz, independent of the train speed. This could be explained by filter effects of the soil with a certain cut-on frequency due to a stiff sub-soil and a certain cut-off frequency due to material damping (fig. 3).

The passage of carriages is analysed in figure 4f to 4j. The characteristics are generally the same as for the locomotive. The dynamic components “sleeper distance” and “soil” are much clearer for the locomotive, so it could be concluded that these components depend on the static axle loads. The low-frequency near-field characteristics, the maxima and minima, are clearer for the regular axle sequence of identical carriages than for the mixed passage of locomotive and carriages. So far, the characteristic frequencies increase with train speed. Only the soil specific component is almost constantly around the layer frequency of 12 Hz.

The amplitudes are increased by a factor of 4 – 10 when the train speed varies between 40 and 160 km/h (fig. 5). That means a relation $A \sim v_T^1 \ldots v_T^{1..5}$. The attenuation with distance is approximately $A \sim r^{-0.7}$ which is a typical value for railway vibration [19, 21]. The geometrical attenuation of elastic surface and body waves is $A \sim r^{-1/2}$ and $A \sim r^{-1}$ for a point load and $A \sim r^0$ and $A \sim r^{-1/2}$ for a line load. Compared to these

theoretic values, the attenuation of the train vibration is rather strong. This experimental result is attributed to the material damping of the soil which yields an additional attenuation of $A \sim e^{-ar}$ for a single harmonic component. Attenuation laws are further discussed in the following section and in [7].

3 Environmental vibration due to explosions

On a large unpopulated test area, explosions with a blast charge of L = 24 to 72 kg have been performed (fig. 6). The vibration of the soil in distances from 10 to 1000 m has been measured in a number of test series. The time records of one example is given in figure 7b. The sandy soil at this site has been analysed by impulse hammer excitation (fig. 7a). Both measurements show a clear propagation of Rayleigh waves with a wave velocity of v_R = 145 – 170 m/s and a wave velocity for the faster compressional wave of v_P = 300 – 360 m/s. The two types of excitation differ in amplitude and frequency content (Fig. 8). The hammer induced vibrations have their maximum at 64 Hz whereas the explosion yields low-frequency vibrations of which the frequency range is reduced with distance from 25 Hz at 10 m to 5 Hz at 1000 m. The vertical impulse excitation of the 5 kg hammer yields good results up to 60 m with a dominant Rayleigh wave. The response to the explosion is different. On the first 100 m, the compressional wave is dominant due to the compressive nature of the excitation. Body waves decrease geometrically by $A \sim r^{-1}$ stronger than surface waves which attenuate geometrically as $A \sim r^{-1/2}$. Therefore, the Rayleigh wave starts to dominate the soil response at 100 m. There is also an attenuation due to material damping of $A \sim e^{-ar}$ which is stronger for slower waves. Therefore, the slower Rayleigh wave is first affected by the damping so that the compressional wave becomes more important at 1000 m once again. Putting all these effects together, figure 9 shows a single power law for the attenuation of $A \sim r^{-1.5}$ for the whole range of distances. It is the result of the superposition of a number of components which attenuate with $A \sim r^{-p} e^{-ar}$ with different p and a. More effects on attenuation laws are studied in Auersch [7].

The amplitudes for thirteen different explosions are in a narrow band (Fig. 9) so that a single law

$$(v/\mathrm{mm/s}) = 264\ (L/\mathrm{kg})^{0.54}\ (r/\mathrm{m})^{-1.25} \qquad (1)$$

for the influence of the blasting charge L and the distance r could be established. The influence of the soil is introduced by the theory of elasticity. The soil at an industrial plant, where bomb clearing must be expected, has been measured by wave methods [22] and found to be stiffer than the soil of the testing area. The prediction curves are shifted down according to the stiffness ratio of the different soils, and the new curves can be compared with the limit values of the German standard DIN 4150 [23] after the multiplication with basic building transfer values. Thus, a good prediction scheme has been established to prevent damage from the buildings of the industrial area.

4 Load and vibration monitoring during drop tests of heavy masses

Drop tests for containers are an important task of the BAM. The dynamics group has made a number of measurements at different drop foundations, with different containers and targets, and for different purposes. First, the rigidity of the foundation had to be proved. Second, the annoyance of residents around the BAM area in Berlin had to be evaluated. Third, the possible damage of a foundation built in an old masonry building has been investigated, and finally, the damage of the foundation for very strong impacts had to be prevented. Usually, singular drops of specific containers on a specific target have been measured. The only systematic variation of the drop height and target stiffness could be performed for the foundation in the masonry building.

4.1 Drop test facility inside an old masonry building

Figure 10 shows the situation within the old masonry building. The building dimensions are V_B = 12 m x 12 m x 12 m where the drop foundation of V_F = 6 m x 6 m x 3.4 m is built inside. The foundation mass is m_F= 300 t, the maximum drop mass is m_C = 8 t and the possible drop height is $h \leq 12$ m. The target area is a steel plate of V_P = 3 m x 2 m x 0.3 m (m_P = 15 t).

On that drop foundation a series of mass drops could be measured with the same drop mass of 1 t. The height varied between 3, 6 and 9.5 m and the target layer was varied between a wooden pallet (soft), a wooden layer (medium), and the bare steel plate (stiff). Figure 11 shows the particle velocities of the foundation for the different mass drops. The results for the soft target (fig. 11a-c) show a first negative half-wave, a second smooth positive half-wave and some attenuating small oscillations. The proportions keep almost constant, but the amplitudes clearly increase with the drop height. If the stiffness of the target is varied in figure 11e-g, the first impulse changes considerably. It gets sharper and some oscillations occur. The second smooth part of the impulse remains almost the same. The maxima of this second smooth part for figure 11a to e are 5.2, 8.1, 10.5, 7.6, and 8.5 mm/s. They are related to the maximum rigid body response, which can be evaluated as

$$v_F \approx \frac{m_C}{m_F} v_C = \frac{1}{300}\sqrt{2gh} = 26, 37, 45\,\text{mm/s} \qquad (2)$$

for the three drop heights h = 3, 6, 9.5 m and a fully plastic impact, (the fully elastic impact would yield twice these amplitudes). These values hold for short impacts, whereas for longer and softer impacts, the decelerating forces of the surrounding soil would get a considerable influence and reduce the maximum velocities. On the other hand, the measurements at the foundation can also include bending and compressional modes and waves namely for the stiff impacts which would yield amplitudes higher than the rigid body estimations.

The absolute maxima for each mass drop and for each group of measurement points are compiled in table 2. The medium and stiff mass drops yield higher amplitudes for the foundation but only moderately increased amplitudes for the wall and the soil responses which seem to follow the base impulse. The amplitudes of the foundation, wall and soil are related approximately as

$$v_F : v_W : v_S \approx 4 : 2 : 1 \qquad (3)$$

in case of the soft impacts. The stiffer impacts have a sharper response with a higher frequency content and yield higher reductions from the foundation to the wall and to the soil.

Subsequently, some drop tests with real containers have been measured and the measured particle velocities of the walls have been compared with the recommendations of the standard DIN4150 [23] to assure the safe performance.

4.2 Drop test facility for heavy mass drops

A test facility for heavy mass drops has been built on the testing area of BAM south of Berlin (fig. 12). The foundation dimension is V = 14 m x 14 m x 5 m, its mass is m_F = 2500 t. The maximum drop mass is m_y = 200 t and the maximum drop height is h = 30 m, where both limits cannot be allowed at the same time. Depending of the softness of the impact, higher drop energies $E = m_C gh$ are possible. To assure the safety of the drop tests, complex measurements have been performed during the first five mass drops.

The monitoring of this big drop test facility of BAM showed the following results for a 127 t steel container dropped from 10 m height. The strain (Fig. 13a), soil stress (Fig. 13b) as well as the (filtered) drop weight acceleration signals display an impulse of $T \approx 60$ ms. This is the most important information as the duration of the impulse includes information of the load that is applied to the drop test foundation. As the total impulse $I = m_C v_C$ = 127 $10^3$14 kgm/s =

$1.8\ 10^6$ kgm/s is brought to zero, the load on the foundation is at least $F \geq I/T = 30$ MN. This minimum value is compared with the other measurement results. The measured strain of $\varepsilon = 80\ \mu$ (fig. 13a) can be related to the stress of $\sigma = 8\ 10^{-5}\ 4\ 10^{10}$ N/m^2 = 3 MN/m^2 with a high elasticity modulus of the reinforced concrete (see below) and to a force of F = 3 MN/m^2 x 10 m^2 = 30 MN with an assumed load area of 10 m^2. The soil stresses under the foundation (fig. 13b) are almost constant σ_S = 120 kN/m^2 on the whole foundation area of A = 196 m^2. The total force on the soil can be calculated as $F_S = pA$ =120 x 196 kN = 24 MN. Thus by the different measurements, the force acting on the drop foundation could be determined quite consistently.

Figure 14 shows the wave propagation through the 5 m thick foundation block. A wave speed of v = 4700 m/s is observed which is much higher than the usual wave velocity of concrete. The higher wave speed is due to the strong reinforcement of the concrete and a special high strength concrete mixture.

Additional sensors (accelerometers and geophones) were used to measure the vibration of the foundation, of the surrounding soil and of the surrounding buildings. Both excitation processes, the release of the mass and the impact, produce high vibration amplitudes. The impact is dominant at the neighbouring tower foundations (fig. 15a, b) whereas the release is dominant for the top tower vibrations (fig. 15c). The mass release excites tower vibrations in its eigen frequency of 10 Hz which comprise several periods until the impact. The ground vibration amplitudes in distances up to 75 m are presented in figure 16. A power law of $A \sim r^{-1.0}$ can clearly be recognized which allows the prediction of building safety in the neighborhood of the drop test facility.

5 Conclusion

Experimental results for train, blast and drop test excitation have been presented for a better understanding of the phenomena. Rules for the prediction of the ground and building vibrations around these normal and extreme excitation processes have been developed. The predicted vibration amplitudes have to be compared with the limit values for annoyance and damage in the standards (for example DIN 4150 [23]).

Acknowledgements

The author wishes to thank his colleagues S. Said, W. Schmid and W. Wuttke for the friendly cooperation at many measurements.

References

[1] Баркан, Д. Динáмика оснований и грунтов. Стройвоэнмориздат, Москва, 1948 (Dynamics of bases and foundations. Mc Graw-Hill, New York, 1962).

[2] Richart, F., Hall, J. and Woods, R. (1970), Vibration of Soils and Foundations, Prentice-Hall, Englewood Cliffs, NJ.

[3] Шахматов Е. Комплексное решение проблем динамики и виброакустики машин. Динамика и виброакустика 1 (2014) 8 С.

[4] Миронова, Т. Разработка конечноэлементной модели виброакустических процессов в трубопроводе с пульсирующим потоком рабочей жидкости. / Т. Миронова, А. Прокофьев, Е. Шахматов. Вестник самарского государственного аэрокосмического университета 3 (2008).

[5] Иголкин, А. О влиянии виброакустических нагрузок на прочность и работоспособность трубопроводных систем. Известия Самарского научного центра Российской академии наук 15 (2013).

[6] Kim, D., Lee, J. Propagation and attenuation characterristics of various ground vibrations. Soil Dynamics Earthquake Engineering 19 (2000) 115-126.

[7] Auersch, L. Technically induced surface wave fields, Part I: Measured attenuation and theoretical amplitude-distance laws. Bulletin of the Seismological Society of America 100 (2010) 1528-1539

[8] Watts, G. The generation and propagation of vibration in various soils

produced by the dynamic loading of road pavements, J. of Sound and Vibration 156 (1992) 191-206.

[9] Auersch, L. Wave propagation in layered soil: theoretical solution in wavenumber domain and experimental results of hammer and railway traffic excitation. Journal of Sound and Vibration 173 (1994) 233-264.

[10] Auersch, L. Technically induced surface wave fields, Part II: Measured and calculated admittance spectra. Bulletin of the Seismological Society of America 100 (2010) 1540-1550.

[11] Dietermann, H., Metrikine, A. The equivalent stiffness of a half-space interacting with a beam. Critical velocities of a load moving along a beam. European J. of Mechanics A/Solids 15 (1996) 67-90.

[12] Krylov, V. Generation of ground vibration boom by high-speed trains. In: V. Krylov (ed.) Noise and Vibration from High-Speed Trains. Telford, London, 2001, 251-283.

[13] Auersch, L. Zur Entstehung und Ausbreitung von Schienenverkehrserschütterungen: Theoretische Untersuchungen und Messungen am Hochgeschwindigkeitszug Intercity Experimental. Forschungsbericht 155, BAM, Berlin, 1988.

[14] Auersch, L., Said, S., Rücker, W. Das Fahrzeug-Fahrweg-Verhalten und die Umgebungserschütterungen bei Eisenbahnen, Forschungsbericht 243, BAM, Berlin, 2001.

[15] Auersch, L. The excitation of ground vibration by rail traffic: Theory of vehicle-track-soil interaction and measurements on high-speed lines. Journal of Sound and Vibration 284 (2005) 103-132.

[16] Maldonado, M. Vibrations dues au passage d'un tramway - mesures expérimentales et simulations numériques, PhD Thesis, École Centrale de Nantes, France, 2008.

[17] Auersch, L., Maldonado, M. Interaction véhicule-voie-sol et vibrations dues aux trains—modélisation et vérifications expérimentales. Revue Européenne de Mécanique Numérique 20 (2011) 257–280.

[18] Alves Costa, P. Vibraçoes do sistema via-maciço induzidas por tráfego ferroviário—modelaçao numérica e validaçao experimental, PhD Thesis, University of Porto, Portugal, 2011.

[19] Romero, A. Predicción, medida experimental y evaluación de las vibraciones producidas por el tráfico ferroviario. PhD Thesis, Universidád de Sevilla, 2012

[20] Auersch, L. Train induced ground vibrations: different amplitude-speed relations for two layered soils. Proceedings of the Institution of Mechanical Engineers, Part F: Journal of Rail and Rapid Transit 226 (2012) 469-488.

[21] Auersch, L. (2014), The use and validation of measured, theoretical and approximated point-load solutions for the prediction of train induced vibration in homogeneous and inhomogeneous soils. International Journal of Acoustics and Vibrations 19(1) (2014) 52-64.

[22] Auersch, L. and Said, S. Comparison of different dispersion evaluation methods and a case history with the inversion to a soil model, related admittance functions, and the prediction of train induced ground vibration. Journal of Near Surface Geophysics 13 (2) (2015) 127-142.

[23] DIN 4150, Erschütterungen im Bauwesen, Teil 3 Einwirkungen auf bauliche Anlagen. Beuth-Verlag, Berlin, 1999.

Appendix

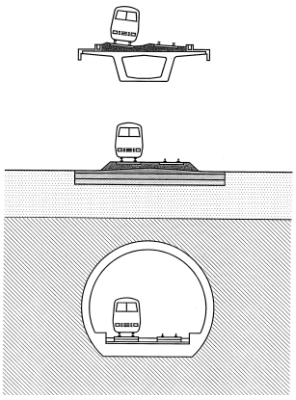

Figure 1. Measurements of railway vibration on a bridge, a surface and a tunnel line

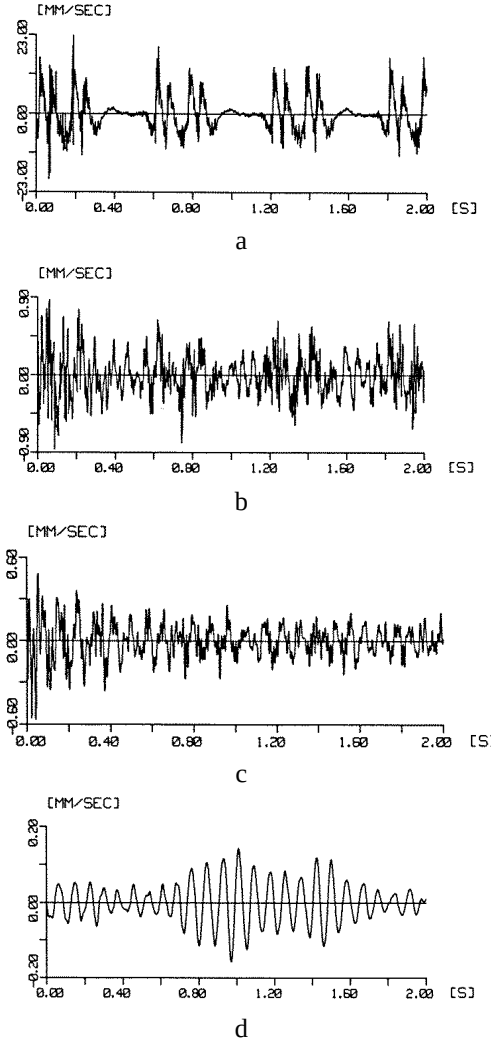

Figure 2. Ground vibration from railway traffic, time records a) at the rail, b) at 2 m, c) 10 m, and d) 100 m distance from the track

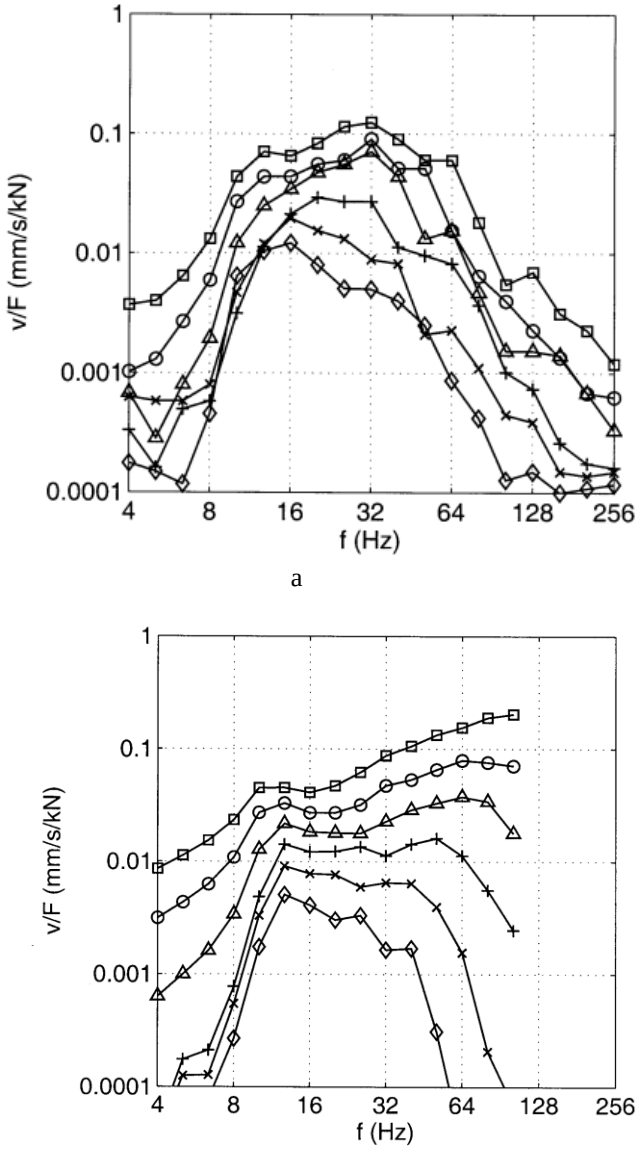

Figure 3. Transfer functions of the soil at distances □ 3, ○ 5, △ 10, + 20, × 30, ◇ 50 m, a) measured near the railway line, b) calculated for a layered soil (shear wave velocities v_{S1} = 270 m/s, v_{S2} = 1000 m/s, layer depth h = 10 m)

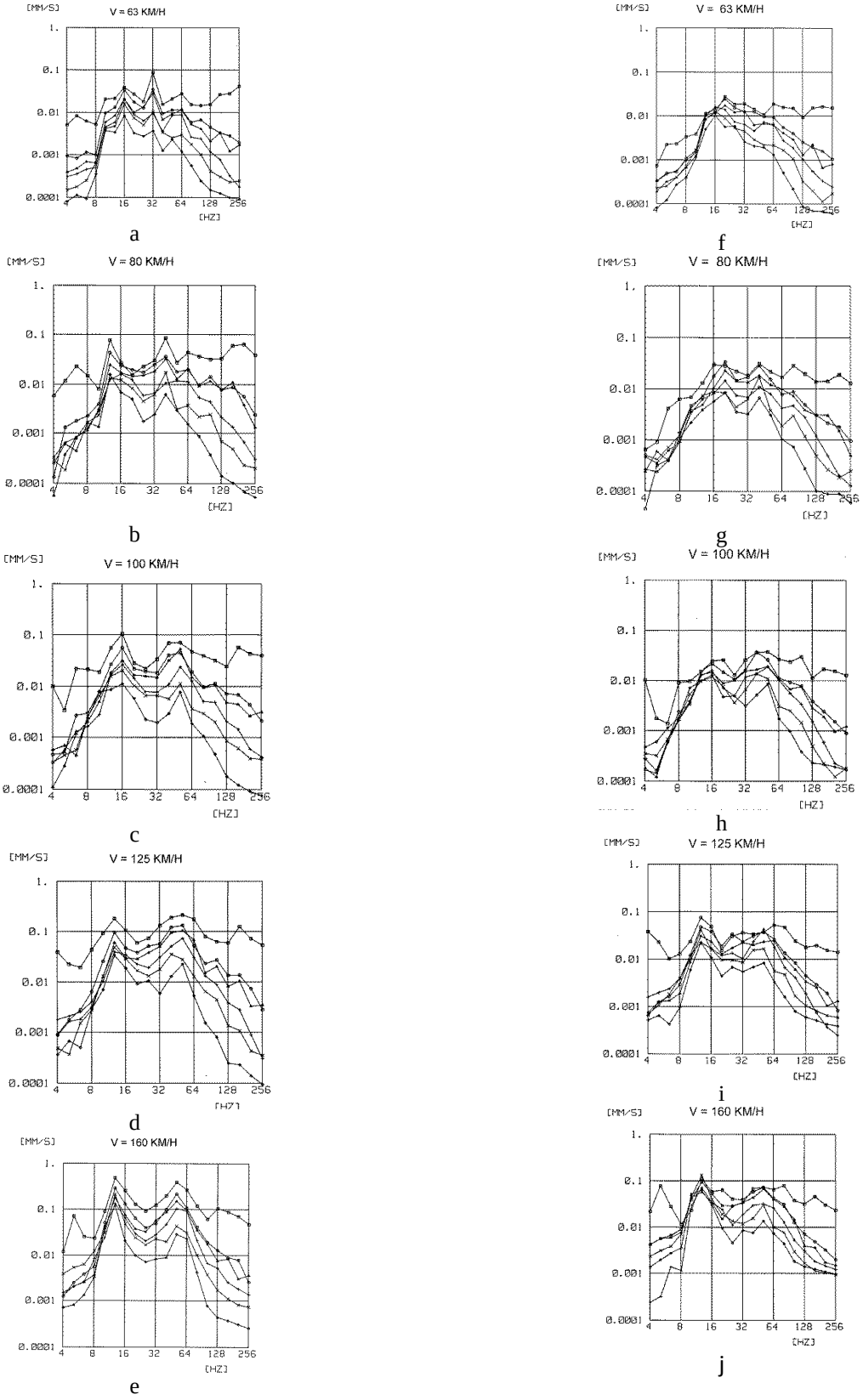

Figure 4. One-third octave band spectra of the train induced ground vibration at distances □ 3, ○ 5, △ 10, + 20, × 30, ◇ 50 m for different train speeds; a, f) 63 km/h; b, g) 80 km/h; c,h) 100 km/h; d, i) 125 km/h; e, j) 160 km/h, locomotive left, carriages right

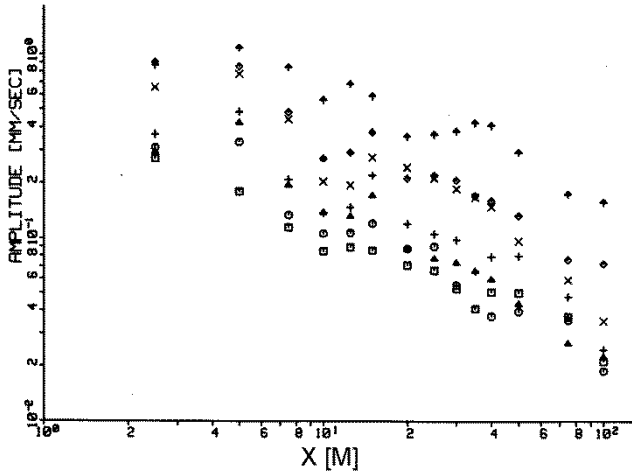

Figure 5. Velocity amplitudes from railway traffic as a function of the distance for different train speeds □ 40, ○ 63, △ 80, + 100, × 125, ◇ 140, ↑ 160 km/h

Figure 6. Explosion on a large unpopulated test area

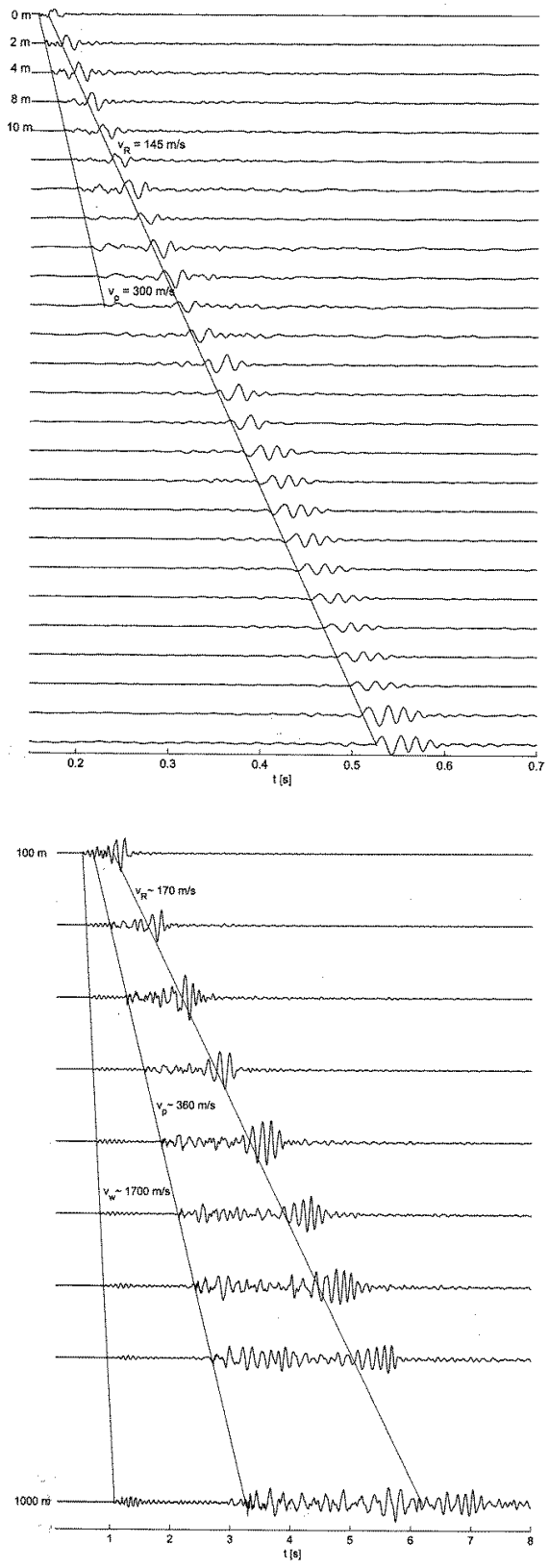

Figure 7. Time records of the ground vibrations due to a) a hammer impact (in 10 to 100 m distance) and b) an explosion (in 100 to 1000 m distance)

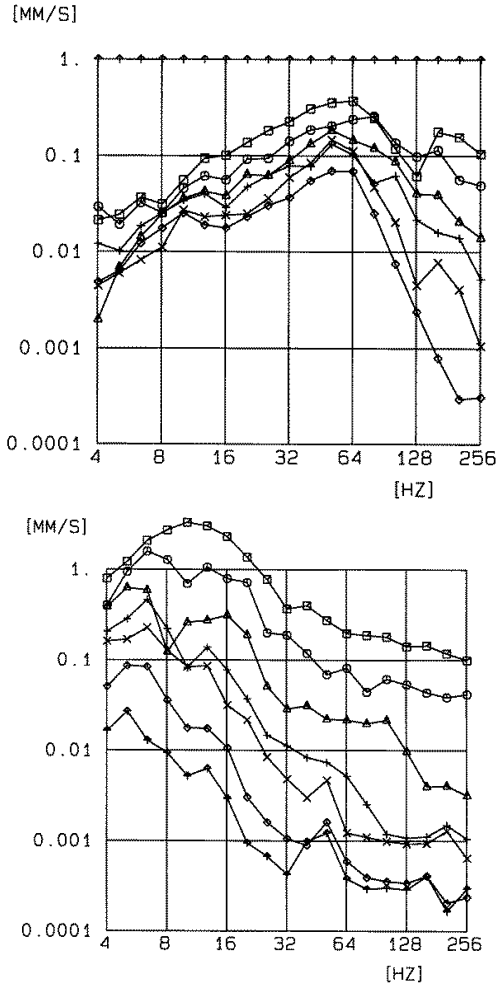

Figure 8. Transfer function of the soil due to hammer impact (left), distances □ 2, ○ 4, △ 8, + 16, × 32, ◇ 54 m, and ground vibration spectra due to explosion (right), distances □ 10, ○ 20, △ 50, + 100, × 200, ◇ 500 m

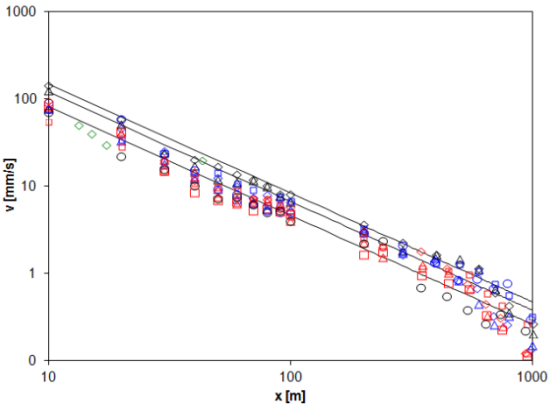

Figure 9. Velocity amplitudes from explosions as a function of the distance for blasting charges of 24, 48 and 72 kg, measurements (markers) and prediction (lines)

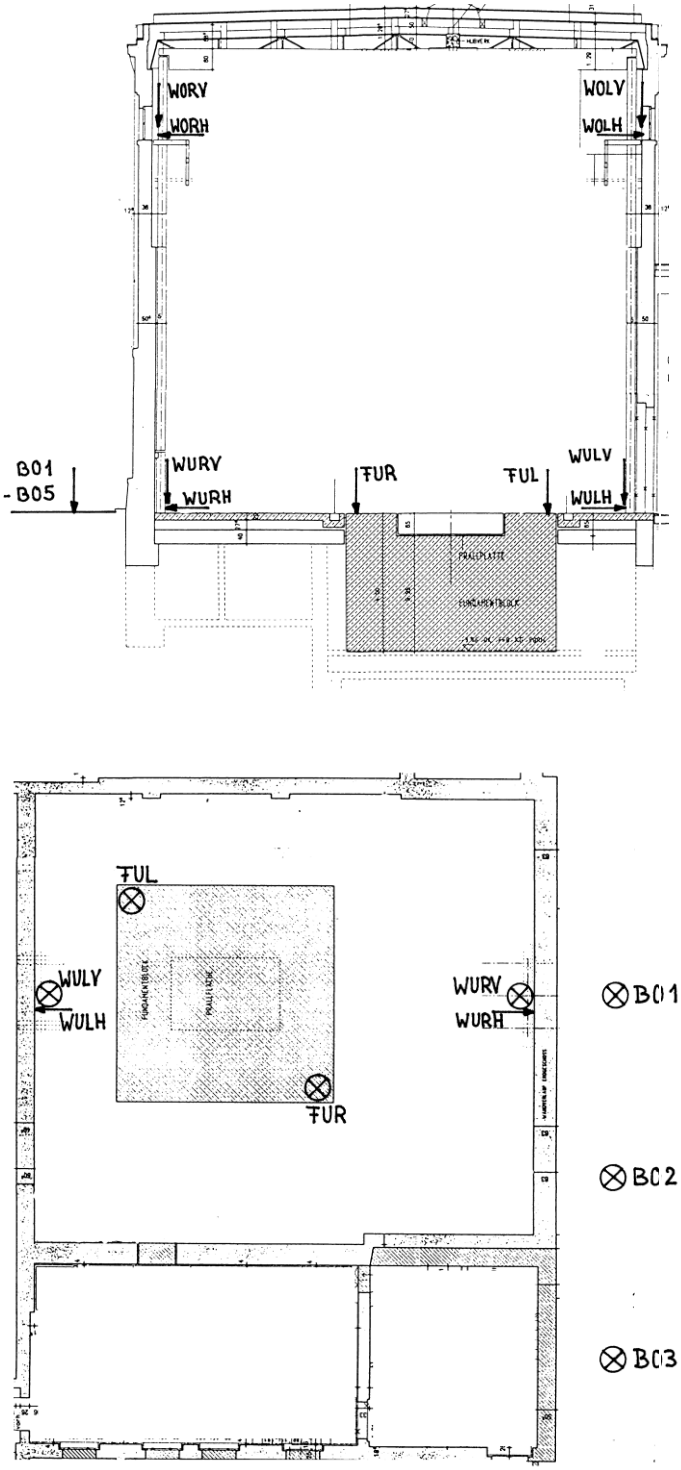

Figure 10. Test facility for mass drops inside a building of BAM, a) view, and b) plan with measuring points

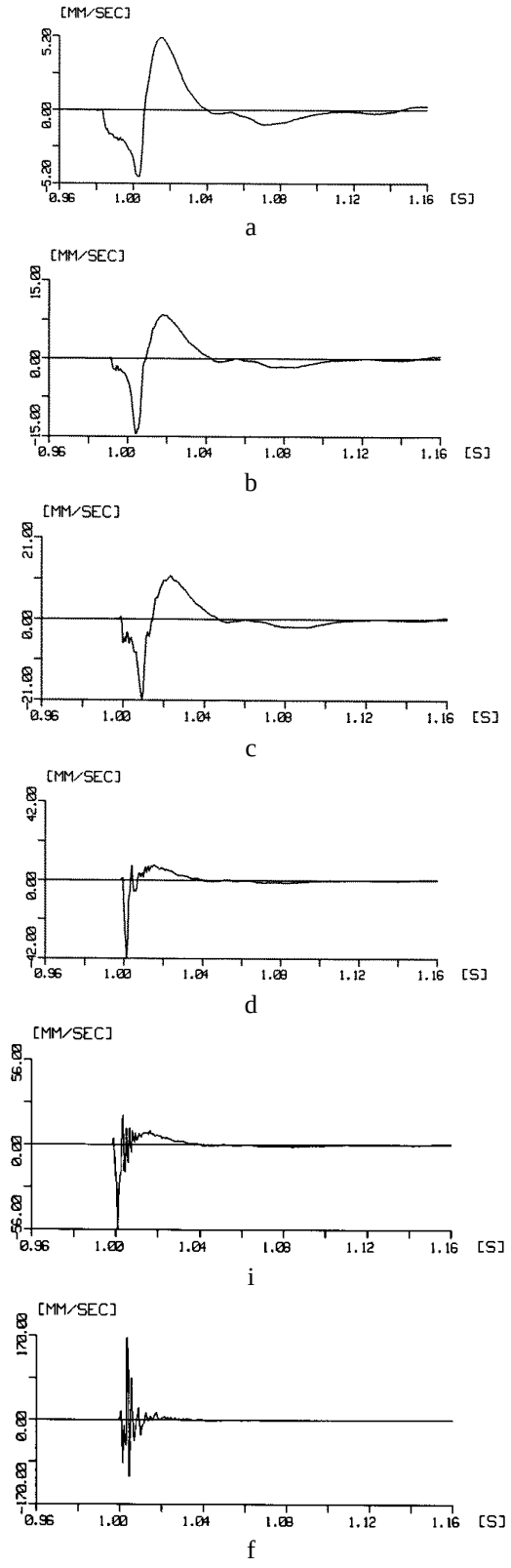

Figure 11. Particle velocities of the foundation, mass drop (m = 1000 kg) from h = a) 3m, b) 6 m, c) 9 m, (on soft target), d) on medium, and e) on stiff target (h = 3 m), f) strongest impact (on stiff target, h = 9 m, m = 500 kg)

a

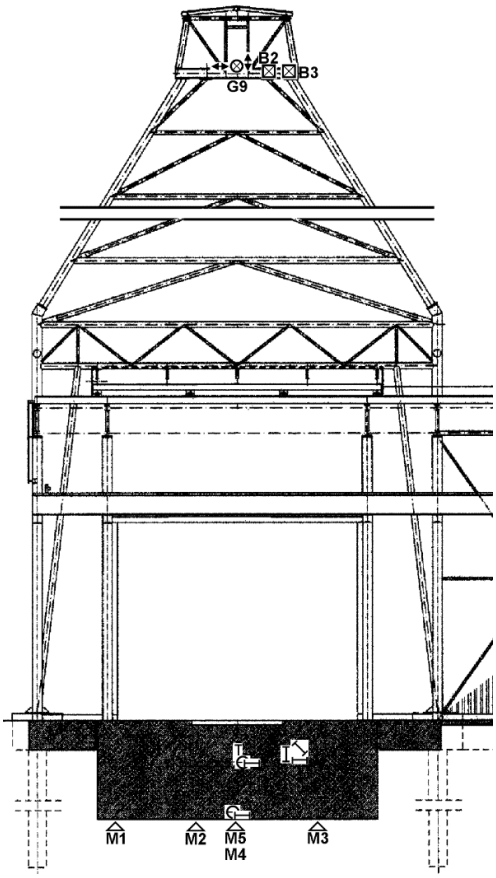

b

Figure 12. Test facility for heavy mass drops at BAM test area, a) view, and b) plan with measuring points

Table 1. Characteristic frequencies for locomotive and carriages (first and second numbers)

Train speed	63 km/h	80 km/h	100 km/h	125 km/h	160 km/h
Near-field maximum 1			-/4 Hz	4/4 Hz	5/5 Hz
Near-field minimum 1		4/4 Hz	5/5-6 Hz	6/6 Hz	8/8 Hz
Near-field maximum 2	5/5 Hz	6/6 Hz	-/8 Hz		12/12 Hz
Sleeper distance	32/- Hz	40/40Hz	50 Hz		
Soil specific part	10-16/-	12/- Hz	16/- Hz	12/12 Hz	12/12 Hz

Table 2. Maximum particle velocity amplitudes for foundation, wall and soil measurement points during drop tests with different drop heights and target stiffnesses

Foundation	3 m	6 m	9.5 m
soft	5.3 mm/s	16.6 mm/s	21.8 mm/s
medium	42.7 mm/s	81.5 mm/s	113.0 mm/s
stiff	55.7 mm/s		*167.0 mm/s
Wall			
soft	4.7 mm/s	8.1 mm/s	9.9 mm/s
medium	6.9 mm/s	15.5 mm/s	18.6 mm/s
stiff	7.7 mm/s		*17.9 mm/s
Soil			
soft	2.2 mm/s	3.8 mm/s	4.5 mm/s
medium	3.5 mm/s	4.6 mm/s	5.4 mm/s
stiff	3.4 mm/s		*3.3 mm/s

* half the drop mass